Optically nonactive assorted helix array with interchangeable magnetic/electric resonance

Xiang Xiong,[1] Xiao-Chun Chen,[1] Mu Wang,[1,a)] Ru-Wen Peng,[1] Da-Jun Shu,[1] and Cheng Sun[2]
[1]*National Laboratory of Solid State Microstructures and Department of Physics, Nanjing University, Nanjing 210093, China*
[2]*Department of Mechanical Engineering, Northwestern University, Evanston, Illinois 60208-3111, USA*

(Received 31 October 2010; accepted 22 January 2011; published online 14 February 2011)

We report here the design of an optically nonactive metamaterial by assembling metallic helices with different chiralities. With linearly polarized incident light, pure electric or magnetic resonance can be selectively realized, which accordingly leads to negative permittivity or negative permeability. Further, we show that pure electric or magnetic resonance can be interchanged at the same frequency band by merely changing the polarization of incident light for 90°. This design demonstrates a unique approach in constructing metamaterials. © *2011 American Institute of Physics*. [doi:10.1063/1.3554704]

The interest in constructing a metamaterial has been promoted by its attractive optical properties, such as negative refractive index,[1–4] ultrahigh spatial resolution,[5,6] invisibility cloaking,[7,8] and optical magnetics.[9,10] These fantastic properties facilitate potential applications in extraordinary optical transmission,[11–15] microscopy,[16] and antennas,[17] etc. Among the massive research in this rapidly developing area, one of the intensively studied subjects is chiral metamaterial, which offers a unique approach to realize negative refractive index.[18–23]

In a chiral metamaterial the strongly coupled electric and magnetic dipoles are simultaneously excited. In previous designs, there usually exists an angle between the electric and the magnetic dipoles, which makes it difficult to fully use the induced dipoles.[19] We once proposed an assembly of double-layered metallic U-shaped resonators with two resonant frequencies ω_H and ω_L.[22,24] The effective induced electric and magnetic dipoles, which originate from the specific distribution of surface electric current upon illumination, are collinear at the same frequency. Despite the efficient use of the electric and magnetic dipoles in that approach, however, the coupling of the building blocks between different layers is very strong, which is not favorable in constructing a three-dimensional bulk metamaterial. One possible solution to deal with this problem is to introduce helix structure.[25] By combining helices with different chiralities, an optically nonactive metamaterial can be constructed.

Here we show that with linearly polarized incident light, pure electric or magnetic resonance can be selectively realized by specific combination of helices of different chiralities. Accordingly, negative permittivity or negative permeability can be achieved.

The elementary building block is a uniaxial gold helix H_1 with three turns, as illustrated in Fig. 1(a). The axis of the helix is along the *x*-direction and the two end points locate in the *x*-*y* plane. The wave vector of incident light is along the *z*-direction and the polarization can be switched in either *x*- or *y*-direction. The commercial software based on the finite difference time domain method (CST MICROWAVE STUDIO) is applied in the simulations. The permittivity of gold in the infrared regime is based on the Drude model, $\varepsilon(\omega)=1-\omega_p^2/(\omega+i\omega_\tau\omega)$, where ω_p is the plasma frequency and ω_τ is the damping constant. For gold, these parameters are taken as $\omega_p=1.37\times10^4$ THz and $\omega_\tau=40.84$ THz.[26] Figure 1(b) shows the transmission coefficients of the array of helix units shown in Fig. 1(a). The distance between the neighboring

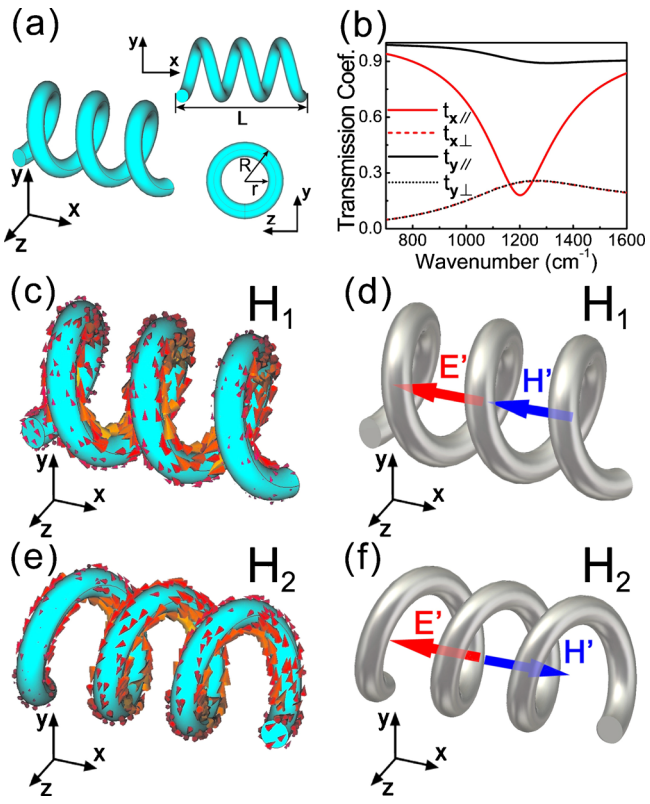

FIG. 1. (Color online) (a) The geometrical parameters of the building block H_1: L=1.0 μm, R=0.25 μm, and r=0.15 μm. (b) Transmission coefficients of an array of H_1 for *x*- and *y*-polarized incidence. (c) and (e) illustrate the calculated induced surface electric current density on H_1/H_2. (d) and (f) schematically show the equivalent electric and magnetic dipoles induced on H_1/H_2.

a)Author to whom correspondence should be addressed. Electronic mail: muwang@nju.edu.cn.

helices in both x- and y-directions is 0.25 μm. The resonant dips in transmission $\mathbf{t}_{\parallel}$, where the polarization of input and output waves is parallel, can be detected at 1200 cm^{-1} for both x-polarized ($\mathbf{t}_{x\parallel}$) and y-polarized ($\mathbf{t}_{y\parallel}$) incidences. The helix possesses intrinsic chirality and the helix array shows optical activity. Consequently resonance peaks of perpendicular polarization of input and output light ($\mathbf{t}_{\perp}$) can be detected in the transmission around 1200 cm^{-1} for both x polarization ($\mathbf{t}_{x\perp}$) and y polarization ($\mathbf{t}_{y\perp}$). Calculations show that $\mathbf{t}_{x\perp}$ and $\mathbf{t}_{y\perp}$ are almost identical [Fig. 1(b)]. It is noteworthy that there exists higher order of resonances in the helix structure, where the induced surface electric current forms a complicated pattern (i.e., the current flows in different directions on different sections of the helix). Here we focus, however, on the lowest frequency resonance of the structure (1200 cm^{-1}), where the induced surface electric current flows in the same direction, as shown in Figs. 1(c) and 1(e). The resonance mode of the surface electric current in the helix does not depend on polarization. The surface current shown in Fig. 1(c) essentially flows along $-x$, which corresponds to an effective electric field $\boldsymbol{E}'$ in $-x$, as indicated by red (light gray) arrow in Fig. 1(d). This means that an effective electric dipole along $-x$ is induced. On the other hand, the surface electric current along helix H_1 forms a loop structure. The curl integration along the projection in the y-z plane is nonzero, which leads to an induced magnetic field $\boldsymbol{H}'$ in $-x$. This indicates that an effective magnetic dipole along $-x$ is induced at the same time, as indicated by the blue (dark gray) arrow in Fig. 1(d).

For a helix with opposite chiralities, H_2 [see Fig. 1(e)], electric and magnetic dipoles can also be excited with both x- and y-polarized incidences, yet the induced electric and magnetic dipoles point to opposite directions roughly, as shown in Fig. 1(f).

The induced surface electric current on the helix contributes not only to the electric/magnetic field along the helix axis (x-direction), but also to very small components in y- and z-directions. Yet those undesired small components of electric/magnetic field can be canceled out by superposing helices with different handedness.[27] The most favorable configuration of the induced electric/magnetic dipoles for optical activity is collinear. To realize such a scenario, we design a structure shown in Fig. 2. The helix H_1 locates in the second quadrant ($-x$,$+y$), with helix axis along the x-direction and the two end points locating in the x-y plane. By taking the y-z plane as the mirror plane, a mirror image of H_1, which possesses the different chirality as H_1, is generated and denoted as H_2. Thereafter, by taking the x-z plane as the mirror plane, two other mirror images, H_2' and H_1', which are the mirror images of H_1 and H_2, respectively, are generated. These four helices are so arranged that x- and y-directions are the symmetry axes of the unit cell. The unit cell is periodically reproduced, and the lattice parameter in the x-direction is 2.5 μm and that in the y-direction is 1.5 μm. When the incident light propagates along the z-direction, the induced resonant surface electric current at 1200 cm^{-1} is illustrated in Fig. 2(a) (x-polarization) and in Fig. 2(b) (y-polarization). For x-polarized incidence, the induced surface electric current in both H_1 (H_1') and H_2 (H_2') moves along the x-direction in general [Fig. 2(a)], and the induced electric dipoles in H_1 (H_1') and H_2 (H_2') are both along x [Fig. 2(c)]. The induced magnetic dipoles of H_1 (H_1') are along x and those of H_2 (H_2') are along $-x$. In other words, the electric dipoles of H_1 (H_1') and H_2 (H_2') are parallel, whereas the magnetic dipoles are antiparallel. Therefore, with such a combination of helices, a pure electric resonance is achieved for x-polarized incidence [Fig. 2(c)].

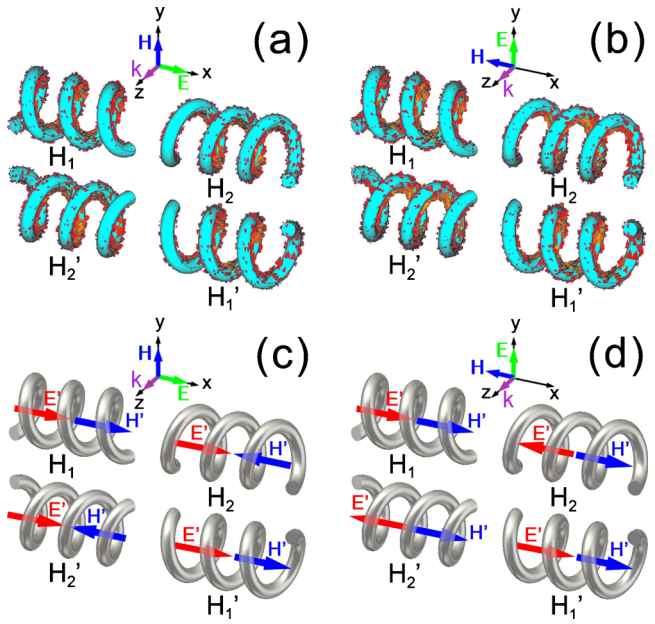

FIG. 2. (Color online) [(a) and (b)] The calculated induced surface electric current density on gold helices when the incident light is polarized in (a) x- and (b) y-directions, respectively. [(c) and (d)] The schematics to show the equivalent electric and magnetic dipoles induced on each building blocks when the incident light is polarized along (c) x- and (d) y-directions, respectively.

For y-polarized incidence, as illustrated in Fig. 2(d), the induced surface electric currents in H_1 (H_1') and H_2 (H_2') move antiparallel along x. So the induced electric dipoles point to the opposite directions, whereas the induced magnetic dipoles are both along x. Therefore, for y-polarized incidence, a pure magnetic resonance is established.

Transmission and reflection coefficients for both x- and y-polarized incidences have been calculated with CST software and are shown in Figs. 3(a) and 3(b), respectively.

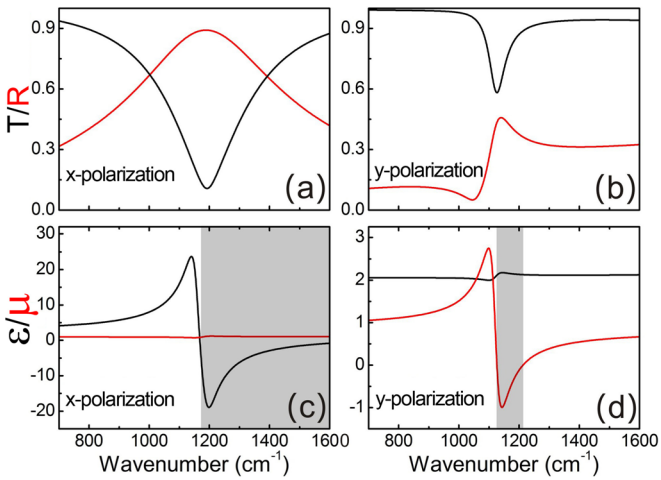

FIG. 3. (Color online) [(a) and (b)] The calculated transmission (T) and reflection (R) coefficients for x/y-polarized incidence. [(c) and (d)] The retrieved effective permittivity (ε) and permeability (μ) for x/y-polarized incidence, respectively. The shaded region corresponds to (c) negative ε and (d) negative μ, respectively.

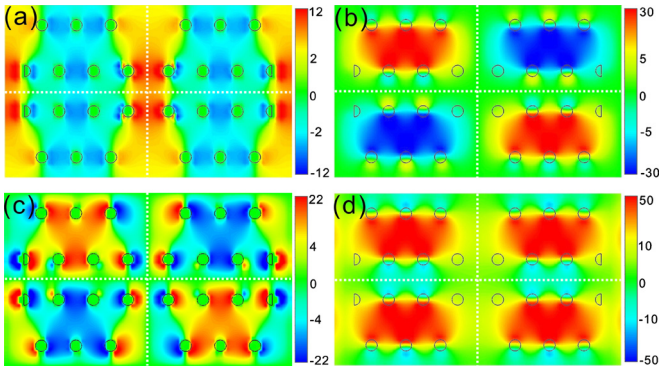

FIG. 4. (Color online) [(a) and (b)] The calculated distribution of x-component of (a) electric and (b) magnetic fields at cross section $z=0$ for x-polarized incidence. [(c) and (d)] The calculated distribution of x-component of (c) electric and (d) magnetic fields at cross section $z=0$ for y-polarized incidence.

Resonant dips in transmissions and peaks in reflections appear between 1100 and 1300 cm^{-1}. Simulation confirms that when the incident light is x- or y-polarized, no energy can be detected in the perpendicular polarization direction. Our calculation also reveals that the transmission and reflection along z- and $-z$-directions are identical. The retrieval method based on S-parameters[28] has been applied to achieve effective permittivity and permeability. Figures 3(c) and 3(d) illustrate the retrieved effective permittivity (ε_{eff}) and permeability (μ_{eff}) of the structure. Pure electric resonance (characterized by an evident jump in ε_{eff}) occurs in 1100–1300 cm^{-1} for x-polarized incidence, and pure magnetic resonance (characterized by an evident jump in μ_{eff}) occurs for y-polarized incidence in the same frequency range. This means that by changing the polarization of incident light, the electric and magnetic resonances of the system can be interchanged.

In order to confirm that pure electric and magnetic resonances really occur as we suggested above, we plot the distribution of x-components of the electric and magnetic fields at the resonant frequencies with x- and y-polarization of incidence, as shown in Fig. 4. The strength of the fields is collected at each point of the x-y plane at $z=0$. The dashed lines divide the unit cell into four regions; in each region a helix with different chirality is placed [the configuration is the same as that in Fig. 2(a)]. For x-polarized incidence [the scenario of Fig. 2(a)], the x-components of the electric field in all the four parts of the unit cell are in phase [Fig. 4(a)], whereas those of the magnetic field are in antiphase and consequently canceled out [Fig. 4(b)]. For y-polarized incidence [the scenario of Fig. 2(b)], the electric field in the four parts of the unit cell is canceled out [Fig. 4(c)], whereas the magnetic field in these parts is in phase and is hence summed up [Fig. 4(d)]. Therefore, Fig. 4 confirms that pure electric resonance indeed occurs when the incident light is x-polarized, while pure magnetic resonance occurs to the same structure when the incident light is switched to y-polarization.

The frequency at which the electric or magnetic resonance occurs depends on the spatial periodicity of the array and the geometrical parameters of the helix itself. Once pure electric or magnetic resonance takes place in the helix array, the resonant frequency decreases as the spatial periodicity is decreased. One may also find that by fixing the other parameters, the resonant frequency shifts to a higher frequency when the length of each helix is shortened. Our unique structural symmetry determines that the pure electric and magnetic resonances can be interchanged at the same frequency by changing the polarization of incident light. This design provides an interesting approach to realize simultaneous magnetic and electric resonances and to construct optically nonactive metamaterials with chiral building blocks.

This work was supported by the State Key Program for Basic Research from the Ministry of Science and Technology of China (Grant No. 2010CB630705), the National Natural Science Foundation of China (Grant Nos. 50972057, 10874068, 11034005, and 61077023), and partly by Jiangsu Province (Grant No. BK2008012).

[1] V. M. Shalaev, Nat. Photonics **1**, 41 (2007).
[2] G. Dolling, M. Wegener, C. M. Soukoulis, and S. Linden, Opt. Lett. **32**, 53 (2007).
[3] S. Zhang, W. J. Fan, N. C. Panoiu, K. J. Malloy, R. M. Osgood, and S. R. J. Brueck, Phys. Rev. Lett. **95**, 137404 (2005).
[4] R. A. Shelby, D. R. Smith, and S. Schultz, Science **292**, 77 (2001).
[5] N. Fang and X. Zhang, Appl. Phys. Lett. **82**, 161 (2003).
[6] J. B. Pendry, Phys. Rev. Lett. **85**, 3966 (2000).
[7] J. B. Pendry, D. Schurig, and D. R. Smith, Science **312**, 1780 (2006).
[8] R. Liu, C. Ji, J. J. Mock, J. Y. Chin, T. J. Cui, and D. R. Smith, Science **323**, 366 (2009).
[9] H. Liu, D. A. Genov, D. M. Wu, Y. M. Liu, Z. W. Liu, C. Sun, S. N. Zhu, and X. Zhang, Phys. Rev. B **76**, 073101 (2007).
[10] T. Q. Li, H. Liu, T. Li, S. M. Wang, F. M. Wang, R. X. Wu, P. Chen, S. N. Zhu, and X. Zhang, Appl. Phys. Lett. **92**, 131111 (2008).
[11] Z. H. Tang, R. W. Peng, Z. Wang, X. Wu, Y. J. Bao, Q. J. Wang, Z. J. Zhang, W. H. Sun, and M. Wang, Phys. Rev. B **76**, 195405 (2007).
[12] W. Wang, Y. L. Lu, R. J. Knize, K. Reinhardt, and S. C. Chen, Opt. Express **18**, 15553 (2010).
[13] Y. J. Bao, R. W. Peng, D. J. Shu, M. Wang, X. Lu, J. Shao, W. Lu, and N. B. Ming, Phys. Rev. Lett. **101**, 087401 (2008).
[14] Y. J. Bao, B. Zhang, Z. Wu, J. W. Si, M. Wang, R. W. Peng, X. Lu, J. Shao, Z. F. Li, X. P. Hao, and N. B. Ming, Appl. Phys. Lett. **90**, 251914 (2007).
[15] Y. J. Bao, H. M. Li, X. C. Chen, R. W. Peng, M. Wang, X. Lu, J. Shao, and N. B. Ming, Appl. Phys. Lett. **92**, 151902 (2008).
[16] A. Salandrino and N. Engheta, Phys. Rev. B **74**, 075103 (2006).
[17] Z. J. Zhang, R. W. Peng, Z. Wang, F. Gao, X. R. Huang, W. H. Sun, Q. J. Wang, and M. Wang, Appl. Phys. Lett. **93**, 171110 (2008).
[18] J. B. Pendry, Science **306**, 1353 (2004).
[19] S. Zhang, Y. S. Park, J. S. Li, X. C. Lu, W. L. Zhang, and X. Zhang, Phys. Rev. Lett. **102**, 023901 (2009).
[20] J. F. Zhou, J. F. Dong, B. N. Wang, T. Koschny, M. Kafesaki, and C. M. Soukoulis, Phys. Rev. B **79**, 121104 (2009).
[21] E. Plum, J. Zhou, J. Dong, V. A. Fedotov, T. Koschny, C. M. Soukoulis, and N. I. Zheludev, Phys. Rev. B **79**, 035407 (2009).
[22] X. Xiong, W. H. Sun, Y. J. Bao, M. Wang, R. W. Peng, C. Sun, X. Lu, J. Shao, Z. F. Li, and N. B. Ming, Phys. Rev. B **81**, 075119 (2010).
[23] B. N. Wang, J. F. Zhou, T. Koschny, and C. M. Soukoulis, Appl. Phys. Lett. **94**, 151112 (2009).
[24] X. Xiong, W. H. Sun, Y. J. Bao, R. W. Peng, M. Wang, C. Sun, X. Lu, J. Shao, Z. F. Li, and N. B. Ming, Phys. Rev. B **80**, 201105(R) (2009).
[25] J. K. Gansel, M. Thiel, M. S. Rill, M. Decker, K. Bade, V. Saile, G. von Freymann, S. Linden, and M. Wegener, Science **325**, 1513 (2009).
[26] M. A. Ordal, R. J. Bell, R. W. Alexander, L. L. Long, and M. R. Querry, Appl. Opt. **24**, 4493 (1985).
[27] D. R. Smith, J. Gollub, J. J. Mock, W. J. Padilla, and D. Schurig, J. Appl. Phys. **100**, 024507 (2006).
[28] D. R. Smith, S. Schultz, P. Markos, and C. M. Soukoulis, Phys. Rev. B **65**, 195104 (2002).